A novel Hsp90 phospho-switch modulates virulence in the major human fungal pathogen *Candida albicans*

Leenah Alaalm[1], Julia L. Crunden[1,2], Mark Butcher[3], Ulrike Obst[2], Ryann Whealy[2], Carolyn E. Williamson[1], Heath E. O'Brien[4], Christiane Schaffitzel[5], Gordon Ramage[3] and Stephanie Diezmann[1,2*]

[1] Department of Biology & Biochemistry, University of Bath, Bath, United Kingdom

[2] School of Cellular and Molecular Medicine, University of Bristol, Bristol, United Kingdom

[3] School of Medicine, Dentistry and Nursing, University of Glasgow, Glasgow, United Kingdom

[4] MRC Centre for Neuropsychiatric Genetics & Genomics, Division of Psychological Medicine & Clinical Neurosciences, Cardiff University, Cardiff, United Kingdom

[5] School of Biochemistry, University of Bristol, Bristol, United Kingdom

Leenah Alaalm and Julia L. Crunden contributed equally to this work.

Running title: Hsp90 phosphorylation modulates *Candida albicans* virulence

Abstract

The ubiquitous molecular chaperone Hsp90 is a key regulator of cellular proteostasis and environmental stress responses. Hsp90 also regulates cellular morphogenesis, drug resistance, and virulence in human pathogenic fungi, which kill more than 1.6 million patients each year worldwide. Invasive fungal infections are difficult to treat due to the lack of effective antifungal therapies, resulting in mortality rates of up to 95%. As a key regulator of fungal virulence, Hsp90 is an attractive therapeutic target. However, fungal and animal homologs are highly conserved, impeding fungal-specific targeting. Thus, understanding the factors that regulate Hsp90 could provide an alternative strategy aimed at exclusively targeting this regulator of fungal virulence. Here, we demonstrate how CK2-mediated phosphorylation of two Hsp90 residues modulates virulence in a major fungal pathogen of humans, *Candida albicans*. We combined proteomics, molecular evolution and structural modelling with molecular biology to identify and characterize two Hsp90 phosphorylation sites. Phosphorylation negatively affects thermal stress response, morphogenesis, drug susceptibility and fungal virulence. Our results provide the first record of specific Hsp90 phosphorylation sites acting as modulators of fungal virulence. Post-translational modifications of Hsp90 could prove valuable in future exploitation as antifungal drug targets.

Introduction

Fungi kill as many patients as tuberculosis and about three times as many as malaria each year[1]. One of the most deadly fungal pathogens, *Candida albicans* causes ~750,000 cases of invasive life-threatening bloodstream infections in immunocompromised patients worldwide each year[1], with mortality rates approaching 75%[2]. In addition to high burdens on human life, fungal infections put a significant strain on health care costs. In 2017, the United States spent $4.5 billion on 75,055 hospitalizations necessitated by fungal disease[3] while English NHS trusts spent more than £90 million on antifungal drugs alone[4]. This already dire situation is further exacerbated by the ever-growing number of patients at risk of contracting invasive fungal infections. It is thus imperative to understand the biological principles underpinning fungal virulence to identify points of fragility suitable for therapeutic targeting.

Diverse aspects of fungal pathogenicity are controlled by heat shock protein 90 (Hsp90), a ubiquitous regulator of the cellular protein homeostasis. Hsp90 regulates cell morphology, drug resistance, and virulence in *C. albicans*[5] and other leading fungal pathogens of humans *Cryptococcus neoformans*[6], which causes brain infections and

57 *Aspergillus fumigatus*[7] which targets the lungs, as well as the dermatophyte *Trichophyton*
58 *rubrum*[8], and *Sporothrix schenckii*[9], the causative agent of cutaneous infections. Hsp90's role
59 in virulence and development is best understood in *C. albicans,* where pharmacological
60 inhibition or genetic reduction of Hsp90 result in reduced drug resistance in planktonic cells[5]
61 and biofilms[10], switching to filamentous growth[11], induction of same-sex mating[12], and
62 delayed cell cycle progression[13]. Although attractive as a drug target for its role in fungal
63 virulence, Hsp90 is highly conserved between mammals and fungi[14]. High sequence
64 conservation prohibits specific targeting of fungal Hsp90 and resulted in severe host toxicity
65 when mice infected with *C. albicans* where treated with Hsp90 inhibitors developed as anti-
66 cancer therapeutics and antifungal drugs[15]. Thus, understanding fungal-specific regulatory
67 mechanisms of Hsp90 could provide an alternative therapeutic approach and is consequently
68 of biological and clinical relevance.

69 Post-translational modifications (PTMs) play a crucial role in regulating Hsp90. Their
70 impact on chaperone activity, directionality of the chaperone cycle, and binding to co-
71 chaperones have been extensively studied in mammalian cells and the model eukaryote
72 *Saccharomyces cerevisiae*[16]. However, examples of Hsp90 PTMs in pathogenic fungi are
73 limited to the observations that concurrent acetylation of two lysine residues, K30 and K271,
74 resulted in increased susceptibility to Hsp90 inhibition, morphogenetic alterations, and
75 impaired macrophage pyroptosis in *C. albicans*[17], as well as attenuated virulence in *A.*
76 *fumigatus*[18]. Given the importance of kinases as drug targets[19] and experimental evidence of
77 phosphorylation regulating most Hsp90 activities, this type of PTM is of particular interest.
78 Phosphorylation negatively affects the chaperone cycle, interactions with clients and co-
79 chaperones, conformational switching, and sensitivity to Hsp90 inhibitors[20]. The ubiquitous
80 tetrameric casein kinase 2 (CK2), one of several kinases targeting Hsp90, phosphorylates
81 $Hsp90^{T36}$ in mammalian cells and $Hsp90^{T22}$ in *S. cerevisiae*. This highly conserved residue
82 was initially identified as critical for the survival of elevated temperatures[21] and
83 phosphorylation of $T^{22/36}$ reduces kinase client stability and co-chaperone binding[22]. In *C.*
84 *albicans*, CK2 phosphorylates Hsp90 serine and threonine residues[23]. Yet, specific Hsp90
85 residues targeted by CK2 and the functional consequences thereof have not been found.

86 Here we demonstrate that CK2-mediated phosphorylation of the newly identified Hsp90
87 residue S530 blocks *C. albicans* virulence and expression of virulence-related traits, such as
88 cellular morphogenesis and survival of thermal stress. Probing the conserved T22 residue
89 revealed that any alteration of this residue leads to loss of Hsp90 function. Our results

90 emphasize the importance of Hsp90 phospho-regulation in fungal virulence and provide a
91 potential site for future therapeutic targeting.
92
93 **Results**
94 **Mapping, modeling, and evolutionary history of CK2 Hsp90 phosphorylation sites.** To
95 map CK2 phosphorylation sites in *C. albicans* Hsp90 *in situ*, the wild-type strain and four
96 mutants, each lacking one CK2 subunit (for strain construction see Tables S1, S2, S3, and
97 Supplementary Information), were grown in rich media at 30˚C upon which epitope tagged
98 Hsp90 was purified and analyzed by mass spectrometry. Without further enrichment, Hsp90
99 sequence coverage in trypsin digests was 70% or higher and ranged between 40-45% in
100 endoproteinase Glu-C digests. Three phosphorylation sites were identified (Table 1). S279
101 was only phosphorylated in the *cka1*Δ/Δ mutant. S294 was phosphorylated in the wild type
102 and all four CK2 mutants. S530 was phosphorylated in the wild type, the *cka1*Δ/Δ and the
103 *ckb1*Δ/Δ mutants, but not the *cka2*Δ/Δ and *ckb2*Δ/Δ mutants. Interestingly, deletion of *CKA2*
104 results in increased fluconazole resistance[24], while Hsp90 inhibition abolishes fluconazole
105 resistance[25].
106 Thus, we hypothesized that phosphorylation of $Hsp90^{S530}$ blocks Hsp90 function,
107 thereby reducing resistance to antifungal drugs. The acquisition of a PTM that reduces drug
108 resistance appears counter-intuitive, but the trade-off theory of optimal virulence predicts
109 selective pressure to evolve reduced virulence in cases where the host and pathogen's fitness
110 are aligned[26]. *C. albicans's* primary ecological niche is as a commensal on mucosal surfaces
111 of the oral cavity and GI tract. To test this, we assessed the effect of $Hsp90^{S530}$
112 phosphorylation on diverse virulence traits, including high temperature growth and
113 morphogenesis.
114 In addition to investigating S530, we decided to also characterize the conserved CK2
115 target $Hsp90^{T22/T36}$, whose *C. albicans* homolog is T25, called T25 henceforth. T25 resides in
116 a highly conserved region of Hsp90's N-terminus, which contains the ATP binding site and is
117 the target of the Hsp90 inhibitors geldanamycin and radicicol[27]. S530 is located in a highly
118 divergent region of the Hsp90 middle domain, where client proteins bind[27] (Fig. 1a). To
119 elucidate the relationship of these two residues within the Hsp90 molecule, we modeled the
120 full-length *C. albicans* Hsp90 monomer on the *S. cerevisiae* crystal structure[28] (Fig. 1b). A
121 total of 609 residues (94% coverage) were aligned with 100% confidence, sharing 89%
122 identity between both yeast species. The homology model revealed that both residues are

123 located in loop regions without secondary structural elements (Fig. 1b). T25 resides in close
124 proximity to the ATP binding pocket, while S530 is located in a loop near the protein's C-
125 terminus. The surface model shows that T25, although not a hydrophobic amino acid, is not
126 solvent exposed, while S530 is (Fig. 1b). These observations are in keeping with molecular
127 evolution theory, which predicts that decreased solvent accessibility results in fewer amino
128 acid polymorphisms[29] and thus higher sequence conservation.

129 Given the divergent nature of the S530 residue (Fig. 1a), we investigated its
130 evolutionary history within the fungal kingdom, asking if *C. albicans* presented a unique case
131 or if multiple transitions could be detected. Aligning 659 amino acids of 240 fungal Hsp90
132 sequences, representing nine sub-phyla, with the murine homolog Hsp90ab1 revealed serine
133 to be a derived allele originating at least eleven times independently within the Dikarya,
134 which encompass the Ascomycota and Basidiomycota, and represent ~96% of known fungal
135 species[30] (Fig. 1c, S1, Table S4). Basal fungi, such as the Chytridiomycota, share an aspartic
136 acid allele with animal cytosolic Hsp90. Threonine originated in the last common ancestor of
137 the Dikarya and threonine to serine transitions were detected in five of the six sub-phyla.
138 Serine alleles were detected in species considered plant pathogens (*Ustilago hordei*, *Puccinia*
139 complex, *Aspergillus niger, Ashbya gossypii*), species associated with trees (*Neolecta*
140 *irregularis*), fermentative yeast (*Nadsonia fulvescens*), methylotrophic yeasts *(Komagataella*
141 *phaffi*, *K. pastoris*, *Ogataea parapolymorpha*, *O. polymorpha*), halo-tolerant species
142 (*Debaryomyces hansenii, Zygosaccharomyces rouxii*) and the opportunistic pathogens
143 (*Meyerozyma guilliermondii*, *Malassezia globosa*, *Candida parapsilosis*). No serine alleles
144 were detected amongst the 82 Agaromycotina, which include the human pathogen
145 *Cryptococcus neoformans* as well as mushrooms and jelly fungi. In summary, the serine allele
146 is rare; it is present in less than 5% of fungi. Serine occurs in species that are capable of
147 causing disease in plants, thrive in extreme environments, and exist as commensals of the
148 human body where they can cause opportunistic infections in responses to changes in the
149 host's immune status, like *C. albicans*.

150 **Hsp90 phosphorylation negatively affects protein stability and co-chaperone binding.** To
151 investigate the effects of phosphorylation of T25 and S530 and to accommodate the 'obligate
152 diploid' nature of *C. albicans*, we generated strains expressing one mutant *hsp90* allele, where
153 the relevant residue was replaced with either a phosphomimetic glutamic acid (E) or a non-
154 phosphorylatable alanine (A) while the remaining *HSP90* wild-type allele was placed under
155 the control of the maltose-inducible promoter *MAL2*p (Tables S1, S2, S3, Supplementary

156 Information). Consequently, strains grown in dextrose solely expressed the mutant allele,
157 thereby revealing the effects of phosphorylation. Growth in maltose resulted in expression of
158 the wild-type allele, serving as control and for strain maintenance. Non-phosphorylatable and
159 phosphomimetic alleles were created for both residues (T25A, T25E, S530A, S530E) and
160 compared to the wild type and the *MAL2-HSP90* promoter control, that carries two *HSP90*
161 wild-type alleles, one of which is under the control of the *MAL2* promoter.

162 To test if phosphorylation affects Hsp90 stability, strains were grown in dextrose or
163 maltose and cell extracts probed for Hsp90 using an antibody that recognizes amino acid
164 residues 693-702 in the *C. albicans* Hsp90 C-terminus[31]. Replacing T25 or S530 with the
165 phosphomimetic residue (E) almost completely depleted Hsp90 levels in cells grown in
166 dextrose when compared to the *MAL2-HSP90* control. Protein levels remained comparable in
167 the strains carrying the non-phosphorylatable alanine allele (A) (Fig. 2a). Thus,
168 phosphorylation of T25 or S530 destabilizes Hsp90.

169 Given the importance of T22/T36 for co-chaperone binding in *S. cerevisiae* and
170 mammalian cells[32], we aimed to determine if the homologous T25 residue plays a similar role
171 in *C. albicans*. Cell lysates from strains with TAP or HA tagged co-chaperones were
172 immunoprecipitated with IgG or α-HA agarose and probed for presence of co-chaperones
173 Cdc37, Aha1, Sba1, and Sti1, which bind to Hsp90's N-terminal domain[33], and for co-
174 immunoprecipitated Hsp90 (Fig. 2b). Changing T25 to either a phosphomimetic or non-
175 phosphorylatable form severely reduced binding of Hsp90 to all four co-chaperones,
176 indicating functional conservation of T25 with regards to co-chaperone binding.

177 **Hsp90 phosphorylation blocks expression of key virulence traits.** Mutational analysis of
178 the *S. cerevisiae* homolog *HSP82* revealed T22 to be essential for survival of elevated
179 temperatures[34], a key virulence trait. To determine the importance of T25 and S530 for
180 growth at high temperatures in *C. albicans*, *hsp90* mutants as well as the wild-type and
181 promoter control strains were spotted onto medium containing either dextrose or maltose and
182 exposed to different temperatures (Fig. 3a). Although neither T25 mutant grew as robust as
183 the wild type or the *MAL2-HSP90* control, the phosphomimetic T25E grew better than the
184 non-phosphorylatable T25A at temperatures above 25˚C. Single colonies were detectable for
185 T25E at the highest dilutions even at 37˚C and 39˚C. Growth of T25A was only detectable at
186 the lowest dilutions at elevated temperatures. In either strain, however, colonies were visibly
187 smaller than in the control suggesting reduced growth rate due to alterations of the T25
188 residue. Growth of the non-phosphorylatable S530A mutant was comparable to the control

189 strains but the phosphomimetic S530E mutant grew much less robust especially at lower
190 temperatures. This suggests phosphorylation of T25 and S530 plays different roles during
191 exposure to thermal stress. Phosphorylation of T25 is required for survival of high
192 temperatures, while phosphorylation of S530 impairs the cell's ability to cope with lower
193 temperatures.

194 Given the importance of Hsp90 in *C. albicans* antifungal drug resistance and the role of
195 Hsp90 PTMs in susceptibility to pharmacological inhibition of Hsp90 function, we tested the
196 phospho-mutants for susceptibility to the commonly used antifungal drug fluconazole and the
197 Hsp90 inhibitor radicicol. Control and phospho-mutant strains were exposed to drug gradients
198 ranging from either 0-256 µg/ml for fluconazole or 0-25 µg/ml for radicicol. Growth was
199 quantified after 48 hours at 25˚C as optical density revealing that expression of *hsp90* mutant
200 alleles sensitizes *C. albicans* to antifungal drug treatment and Hsp90 inhibition (Fig. 3b).
201 Changing T25 to either a phosphomimetic or non-phosphorylatable allele or expressing the
202 S530 phospho-allele rendered *C. albicans* susceptible to either drug. This suggests Hsp90
203 phosphorylation to be a determinant of drug susceptibility.

204 Cellular morphogenetic diversity is a fundamental element of *C. albicans'* virulence
205 repertoire as the ability to switch between yeast and hyphae is essential for the infectious
206 process[35]. To determine how phosphorylation of T25 or S530 affects cellular morphogenesis,
207 the wild type, the *MAL2-HSP90* control and the *hsp90* mutants were grown in standard non-
208 filament inducing conditions in rich media at 30˚C. Microscopic examination of planktonic
209 cells showed robust hyphal growth in both T25 mutants as well as the S530E strain in media
210 containing dextrose, but not maltose (Fig. 3c). To quantify these observations, we calculated
211 the morphology index (MI) for 100 randomly selected cells for each strain (Fig. S2). An MI >
212 1 is indicative of cell elongation or hyphal growth. MI scores for cells grown in dextrose or
213 maltose differed significantly for both T25 mutants and S530E. In maltose, MIs clustered
214 below 1, in dextrose MIs ranged from ~0.2 to ~75. Hence, both T25 mutant alleles and the
215 phosphomimetic S530E allele cause cells to switch from yeast to hyphal growth.

216 **Hsp90's phosphorylation status affects colony appearance and biofilm viability.**
217 Following up on the observation that differential Hsp90 phosphorylation results in elongated
218 cell shape, we assessed macroscopic changes to colony morphology and response to cell wall
219 stress. To capture changes in colony morphology, all strains were grown on nutrient-limited
220 RPMI, synthetic defined (SD) media alone and supplemented with Calcofluor White or
221 Congo Red as well as Spider media, which induces the yeast-to-hyphae transition (Table S5).

222 Upon visual inspection of plates grown for 48 hours at 30˚C, wild-type colonies were
223 indistinguishable from the *MAL2-HSP90* control (Fig. 4). Colonies for both T25 mutants and
224 the S530E strain appeared different from controls on RPMI and SD media. Despite being
225 highly filamentous on a cellular level, colonies of these strains lost their hyphal edge on
226 RPMI. On SD, these colonies were wrinkly rather than smooth. Growth on maltose restored
227 wild type-like growth on RPMI and, to a degree, on SD media. No appreciable differences
228 were observed for colonies grown in the presence of Congo Red or Calcofluor White when
229 compared to SD only media (data not shown). Differences in colony morphology on Spider
230 media appeared to be driven by the carbon source rather than a strain's *HSP90* allele.

231 Morphogenetic diversity is a key prerequisite for the formation of *C. albicans* biofilms,
232 which are medically relevant for two reasons. First, biofilms act as reservoirs that
233 continuously feed the infection, and secondly they are intrinsically resistant to treatment with
234 antifungal drugs[36]. To determine if Hsp90's phosphorylation status affects the intricate
235 developmental program underlying biofilm formation, cells were grown in standard biofilm-
236 inducing conditions in RPMI (2 g/l glucose) at 37˚C. Mature biofilms were imaged using
237 scanning electron microscopy and their cell viability and biomass were quantified employing
238 spectrometric approaches. Microscopic analysis of biofilm architecture at 800x and 8,000x
239 magnifications showed that control strains and phospho-mutants form structurally similar
240 biofilms, suggesting that Hsp90's phosphorylation status does not fundamentally affect
241 overall biofilm development in the conditions tested (Fig. 5a). More detailed inspection of
242 biomass production and cell viability revealed that the latter is significantly decreased in the
243 S530E mutant ($p=0.00205$) relative to the *MAL2-HSP90* control (Fig. 5b, c). This is in
244 keeping with previous observations of phosphorylation of $Hsp90^{S530}$ resulting in a loss-of-
245 function phenotype. All other phospho-mutants displayed significant increases in cell viability
246 (T25A: $p=4.01x10^{-14}$; T25E: $p=9.94x10^{-13}$; S530A: $p=8.68x10^{-7}$). While deviating from our
247 observation of a growth defect in the T25 mutants at 37˚C on YPD agar, Azadmanesh *et al.*
248 have shown that the physical environment influences *C. albicans* gene expression and
249 development[37].

250 Building on our finding that Hsp90's phosphorylation status determines its effect on *C.*
251 *albicans* cellular morphogenesis, we demonstrated that phosphorylation of S530 results in
252 changes in colony morphology and reduced biofilm cell viability due to loss of Hsp90
253 function. Any manipulation of the T25 residue, however, leads to elongated cells, aberrant
254 colony morphology and increased biofilm cell viability.

255 **S530 regulates *C. albicans* virulence in an invertebrate model of fungal pathogenesis.**
256 Once we established the importance of phosphorylation of S530 and T25 in virulence-relevant
257 traits using different *in vitro* assays, we aimed to determine if and how Hsp90
258 phosphorylation affects fungal virulence. To test this, *Manduca sexta* caterpillars, an
259 invertebrate model host of fungal disease[38], were infected with 10^7 yeast cells. Caterpillar
260 survival was then assessed in groups of ten after 16 hours of incubation at the physiologically
261 relevant temperature of 37˚C. Strain S530E displayed significantly reduced virulence
262 compared to the *MAL2-HSP90* control (Table S6). Nine caterpillars infected with S530E
263 survived compared to two caterpillars infected with *MAL2-HSP90* (p=0.0054775). Thus,
264 S530 phosphorylation blocks Hsp90 function, thereby attenuating virulence in an animal host.

265 In summary, Hsp90's phosphorylation status affects fungal virulence. Taken together,
266 our results suggest that S530 is a novel phospho-switch. When phosphorylated, it blocks
267 Hsp90 function and thus the expression of virulence traits, which may aid its adaptation to a
268 commensal lifestyle while maintaining the ability to cause invasive infections. Alterations of
269 T25, however, are important beyond phosphorylation, suggesting this residue to be a 'switch
270 point', important for structural integrity of *C. albicans* Hsp90.

271

272 **Discussion**

273 Our data indicate that CK2-mediated phosphorylation of $Hsp90^{S530}$ blocks expression of
274 virulence traits in a major human pathogen while any alteration of $Hsp90^{T25}$ resulted in a loss-
275 of-function phenotype. This suggests that S530 is a novel *C. albicans* Hsp90 phospho-switch
276 while T25 acts as switch point.

277 Similarly, to what has been observed in *S. cerevisiae* and mammalian cells, any
278 modification of *C. albicans* T25 negatively affects co-chaperone binding, survival of high
279 temperatures, and susceptibility to drug and Hsp90 inhibition[32,39]. We thus propose that T25
280 acts as a switch point in *C. albicans* Hsp90. Switch points impact on the overall conformation
281 and function of a protein through conformational disturbances altering chaperone function[40].
282 These types of allosteric PTMs are of evolutionary significance as they expand the
283 proteome's complexity and facilitate dynamic responses to a large number of stimuli without
284 the need for additional genes[41]. The effect, however, appears to be restricted to T22 in *S.*
285 *cerevisiae* and T25 in *C. albicans*, as changes in the acetylation status of the neighboring
286 conserved *C. albicans* K30[17] or *S. cerevisiae* K27[42] residues did not result in loss of Hsp90
287 function.

288 Detection of phosphorylation of S530 has remained rather elusive. Only one[43] of five
289 global phospho-proteomic analyses of *C. albicans*[44-47] detected phosphorylation of Hsp90^{S530}
290 in *C. albicans* hyphal cells[43]. This finding is consistent with our experimental data showing
291 filamentous growth in the phosphomimetic S530E mutant. While our proteomic analysis
292 revealed S530 to be phosphorylated in the wild type, the wild-type and *MAL2-HSP90* control
293 are phenotypically more similar non-phosphorylatable mutant S530A than the they are to
294 phosphomimetic mutant S530E (Fig. 3). This would suggest that phosphorylation of S530 is
295 sparsely deployed and dynamic. Characterizing the *S. cerevisiae* homologous residue T533
296 using phosphomimetic and non-phosphorylatable alleles revealed that this residue does not
297 affect survival at elevated temperatures, susceptibility to Hsp90 inhibition, or yeast growth[48]
298 suggesting evolutionary divergence in sequence and function. Taken together, the dynamic
299 phosphorylation status of S530 carefully orchestrating *C. albicans* virulence in a commensal
300 turned pathogen yeast and the lack of involvement in Hsp90 function of T533 in the benign
301 yeast *S. cerevisiae* would be in keeping with S530 to be a genetic factor that reduces severity
302 as predicted by the trade-off hypothesis of optimal virulence theory.

303 In conclusion, Hsp90's phosphorylation status and structural integrity affect fungal
304 virulence. CK2-mediated phosphorylation of the divergent S530 residue resulting in reduced
305 fungal virulence could be further exploited as a novel therapeutic target to fight fungal
306 infections.

307

308 **References**

309 1. Bongomin, F., Gago, S., Oladele, R. & Denning, D. Global and multi-national
310 prevalence of fungal diseases - estimate precision. *JoF* **3,** 57–29 (2017).
311 2. Brown, G. D. *et al.* Hidden killers: Human fungal infections. *Sci Transl Med* **4,**
312 165rv13 (2012).
313 3. Benedict, K., Jackson, B. R., Chiller, T. & Beer, K. D. Estimation of direct healthcare
314 costs of fungal diseases in the United States. *Clin Infect Dis* **30,** 1 (2018).
315 4. Whitney, L. *et al.* Effectiveness of an antifungal stewardship programme at a London
316 teaching hospital 2010–16. *J Antimicrob Chemother* **74,** 234–241 (2018).
317 5. Singh, S. D. *et al.* Hsp90 governs echinocandin resistance in the pathogenic yeast
318 *Candida albicans* via calcineurin. *PLoS Pathog* **5,** e1000532 (2009).
319 6. Cordeiro, R. de A. *et al.* Inhibition of heat shock protein 90 enhances the susceptibility
320 to antifungals and reduces the virulence of *Cryptococcus neoformans*/*C. gattii* species
321 complex. *Microbiology* **162,** 309–317 (2015).
322 7. Lamoth, F., Juvvadi, P. R., Fortwendel, J. R. & Steinbach, W. J. Heat shock protein 90
323 is required for conidiation and cell wall integrity in *Aspergillus fumigatus*. *Eukaryot*
324 *Cell* **11,** 1324–1332 (2012).
325 8. Jacob, T. R. *et al.* Heat shock protein 90 (Hsp90) as a molecular target for the

326 development of novel drugs against the dermatophyte *Trichophyton rubrum*. *Front*
327 *Microbiol* **6,** 330–10 (2015).
328 9. Rodriguez-Caban, J., Gonzalez-Velazquez, W., Perez-Sanchez, L., Gonzalez-Mendez,
329 R. & Valle, N. R.-D. Calcium/calmodulin kinase1 and its relation to thermotolerance
330 and HSP90 in *Sporothrix schenckii*: an RNAi and yeast two-hybrid study. *BMC*
331 *Microbiol* **11,** 162 (2011).
332 10. Robbins, N. *et al.* Hsp90 governs dispersion and drug resistance of fungal biofilms.
333 *PLoS Pathog* **7,** e1002257 (2011).
334 11. Shapiro, R. S. *et al.* Hsp90 orchestrates temperature-dependent *Candida albicans*
335 morphogenesis via Ras1-PKA signaling. *Curr Biol* **19,** 621–629 (2009).
336 12. Guan, G. *et al.* Environment-induced same-sex mating in the yeast *Candida albicans*
337 through the Hsf1–Hsp90 pathway. *PLoS Biol.* **17,** e2006966–25 (2019).
338 13. Senn, H., Shapiro, R. S. & Cowen, L. E. Cdc28 provides a molecular link between
339 Hsp90, morphogenesis, and cell cycle progression in *Candida albicans*. *Mol Biol Cell*
340 **23,** 268–283 (2012).
341 14. Swoboda, R. K. *et al.* Structure and regulation of the *HSP90* gene from the pathogenic
342 fungus *Candida albicans*. *Infect Immun* **63,** 4506–4514 (1995).
343 15. Cowen, L. E. *et al.* Harnessing Hsp90 function as a powerful, broadly effective
344 therapeutic strategy for fungal infectious disease. *PNAS* **106,** 2818–2823 (2009).
345 16. Mollapour, M. & Neckers, L. Post-translational modifications of Hsp90 and their
346 contributions to chaperone regulation. *BBA* **1823,** 648–655 (2012).
347 17. Li, X., Robbins, N., O'Meara, T. R. & Cowen, L. E. Extensive functional redundancy
348 in the regulation of *Candida albicans* drug resistance and morphogenesis by lysine
349 deacetylases Hos2, Hda1, Rpd3 and Rpd31. *Mol Microbiol* **103,** 635–656 (2016).
350 18. Lamoth, F. *et al.* Identification of a key lysine residue in heat shock protein 90 required
351 for azole and echinocandin resistance in *Aspergillus fumigatus*. *Antimicrob Agents*
352 *Chemother* **58,** 1889–1896 (2014).
353 19. Cohen, P. Protein kinases - the major drug targets of the twenty-first century? *Nat Rev*
354 *Drug Discov* **1,** 309–315 (2002).
355 20. Sima, S. & Richter, K. Regulation of the Hsp90 system. *BBA-Mol Cell Res* **1865,** 889–
356 897 (2018).
357 21. Borkovich, K. A., Farrelly, F. W., Finkelstein, D. B., Taulien, J. & Lindquist, S. hsp82
358 is an essential protein that is required in higher concentrations for growth of cells at
359 higher temperatures. *Mol Cell Biol* **9,** 3919–3930 (1989).
360 22. Lees-Miller, S. Two human 90-kDa heat shock proteins are phosphorylated *in vivo* at
361 conserved serines that are phosphorylated *in vitro* by casein kinase II. *J Biol Chem*
362 (1989).
363 23. Diezmann, S., Michaut, M., Shapiro, R. S., Bader, G. D. & Cowen, L. E. Mapping the
364 Hsp90 genetic interaction network in *Candida albicans* reveals environmental
365 contingency and rewired circuitry. *PLoS Genet* **8,** e1002562 (2012).
366 24. Bruno, V. M. Regulation of azole drug susceptibility by *Candida albicans* protein
367 kinase CK2. *Mol Microbiol* **56,** 559–573 (2005).
368 25. Cowen, L. E. & Lindquist, S. Hsp90 potentiates the rapid evolution of new traits: drug
369 resistance in diverse fungi. *Science* **309,** 2185–2189 (2005).
370 26. Ewald, P. W.1983. Host-parasite relations, vectors, and the evolution of disease
371 severity. *Ann Rev Ecol Syst* **14,** 465–485 (1983).
372 27. Pearl, L. H. & Prodromou, C. Structure and mechanism of the Hsp90 molecular
373 chaperone machinery. *Annu Rev Biochem* **75,** 271–294 (2006).
374 28. Ali, M. M. U. *et al.* Crystal structure of an Hsp90–nucleotide–p23/Sba1 closed
375 chaperone complex. *Nature* **440,** 1013–1017 (2006).

29. Bustamante, C. D., Townsend, J. P. & Hartl, D. L. Solvent accessibility and purifying selection within proteins of *Escherichia coli* and *Salmonella enterica*. *Mol Biol Evol* **17,** 301–308 (2000).
30. Blackwell, M. The Fungi: 1, 2, 3 … 5.1 million species? *Am J Bot* **98,** 426–438 (2011).
31. Burt, E. T. *et al.* Isolation and partial characterization of Hsp90 from *Candida albicans*. *Ann Clin Lab Sci* **33,** 86–93 (2003).
32. Mollapour, M. *et al.* Threonine 22 phosphorylation attenuates Hsp90 interaction with cochaperones and affects its chaperone activity. *Mol Cell* **41,** 672–681 (2011).
33. Röhl, A., Rohrberg, J. & Buchner, J. The chaperone Hsp90: changing partners for demanding clients. *Trends Biochem Sci* **38,** 253–262 (2013).
34. Nathan, D. F. & Lindquist, S. Mutational analysis of Hsp90 function: interactions with a steroid receptor and a protein kinase. *Mol Cell Biol* **15,** 3917–3925 (1995).
35. Saville, S. P., Lazzell, A. L., Monteagudo, C. & Lopez-Ribot, J. L. Engineered control of cell morphology *in vivo* reveals distinct roles for yeast and filamentous forms of *Candida albicans* during infection. *Eukaryot Cell* **2,** 1053–1060 (2003).
36. Lagree, K. & Mitchell, A. P. Fungal biofilms: Inside out. *Microbiol Spectr* **5,** 1–22 (2017).
37. Azadmanesh, J., Gowen, A. M., Creger, P. E., Schafer, N. D. & Blankenship, J. R. Filamentation involves two overlapping, but distinct, programs of filamentation in the pathogenic fungus *Candida albicans*. *G3 (Bethesda)* **7,** 3797–3808 (2017).
38. Lyons, N. *et al.* Tobacco Hornworm (*Manduca sexta*) caterpillars as a novel host model for the study of fungal virulence and drug efficacy. *Virulence* **11,** 1075–1089 (2020).
39. Mollapour, M., Tsutsumi, S., Kim, Y. S., Trepel, J. & Neckers, L. Casein kinase 2 phosphorylation of Hsp90 threonine 22 modulates chaperone function and drug sensitivity. *Oncotarget* **2,** 407–417 (2011).
40. Rehn, A. *et al.* A methylated lysine is a switch point for conformational communication in the chaperone Hsp90. *Nat Commun* **11,** 1–14 (2020).
41. Nussinov, R., Tsai, C.-J., Xin, F. & Radivojac, P. Allosteric post-translational modification codes. *Trends Biochem Sci* **37,** 447–455 (2012).
42. Robbins, N., Leach, M. D. & Cowen, L. E. Lysine deacetylases Hda1 and Rpd3 regulate Hsp90 function thereby governing fungal drug resistance. *Cell Reports* **2,** 878–888 (2012).
43. Willger, S. D. *et al.* Analysis of the *Candida albicans* phosphoproteome. *Eukaryot Cell* **14,** 474–485 (2015).
44. Ghorai, P., Irfan, M., Narula, A. & Datta, A. A comprehensive analysis of *Candida albicans* phosphoproteome reveals dynamic changes in phosphoprotein abundance during hyphal morphogenesis. *Appl Microbiol Biotechnol* **102,** 1–13 (2018).
45. Bar-Yosef, H. *et al.* A global analysis of kinase function in *Candida albicans* hyphal morphogenesis reveals a role for the endocytosis regulator Akl1. *Front Cell Infect Microbiol* **8,** 1538–13 (2018).
46. Vlastaridis, P. *et al.* The pivotal role of protein phosphorylation in the control of yeast central metabolism. *G3 (Bethesda)* **7,** 1239–1249 (2017).
47. Cao, C. *et al.* Global regulatory roles of the cAMP/PKA pathway revealed by phenotypic, transcriptomic and phosphoproteomic analyses in a null mutant of the PKA catalytic subunit in *Candida albicans*. *Mol Microbiol* **105,** 46–64 (2017).
48. Soroka, J. *et al.* Conformational switching of the molecular chaperone Hsp90 via regulated phosphorylation. *Mol Cell* **45,** 517–528 (2012).
49. Pereira, F. *et al.* Effect of Sec61 interaction with Mpd1 on endoplasmic reticulum-associated degradation. *PLoS ONE* **14,** e0211180–19 (2019).

50. Mezulis, S., Yates, C. M., Wass, M. N., Sternberg, M. J. E. & Kelley, L. A. The Phyre2 web portal for protein modeling, prediction and analysis. *Nat Protoc* 1–14 (2019).
51. Schrödinger, L. L. C. The PyMOL Molecular Graphics System.
52. Larsson, A. AliView: a fast and lightweight alignment viewer and editor for large datasets. *Bioinformatics* **30,** 3276–3278 (2014).
53. Edgar, R. C. MUSCLE: multiple sequence alignment with high accuracy and high throughput. *Nucleic Acid Res* **32,** 1792–1797 (2004).
54. Kumar, S., Stecher, G., Li, M., Knyaz, C. & Tamura, K. MEGA X: Molecular Evolutionary Genetics Analysis across computing platforms. *Mol Biol Evol* **35,** 1547–1549 (2018).
55. Maddison, W. P. & Maddison, D. R. Mesquite: a modular system for evolutionary analysis.
56. Mersondavies, L. A. & Odds, F. C. A morphology index for characterization of cell-shape in *Candida albicans*. *J Gen Microbiol* **135,** 3143–3152 (1989).
57. Schneider, C. A., Rasband, W. S. & Eliceiri, K. W. NIH Image to ImageJ: 25 years of image analysis. *Nat Methods* **9,** 671 EP –
58. Saldanha, A. J. Java Treeview - extensible visualization of microarray data. *Bioinformatics* **20,** 3246–3248 (2004).
59. Sherry, L. *et al.* Biofilms formed by *Candida albicans* bloodstream isolates display phenotypic and transcriptional heterogeneity that are associated with resistance and pathogenicity. *BMC Microbiol* **14,** 182 (2014).
60. Erlandsen, S. L., Kristich, C. J., Dunny, G. M. & Wells, C. L. High-resolution visualization of the microbial glycocalyx with low-voltage scanning electron microscopy: Dependence on cationic dyes. *J Histochem Cytochem.* **52,** 1427–1435 (2016).

453 **Methods**

454 **Strains, strain construction and culture conditions.** All strains used in this study are listed
455 in Table S1. A detailed description of strain and plasmid construction can be found in the
456 Supplementary Information together with Tables S2 and S3, which list the necessary primers.
457 In preparation for experiments, strains were grown for 16-18 hours in YPM (1% yeast extract,
458 2% peptone, 2% maltose) at 30˚C while shaking at 200 rpm, unless specified otherwise. To
459 repress the *HSP90* wild-type allele, strains were grown in YPD (1% yeast extract, 2%
460 peptone, 2% dextrose) at the temperatures specified. For long-term storage, strains were
461 maintained at -80˚C in 25% glycerol.

462 **Identification of the S530 phosphorylation site.** The S530 phosphorylation site in Hsp90
463 was identified by mass spectrometric analysis of purified Hsp90 in the Proteomics Core
464 Facility at EMBL Heidelberg, Germany. To purify Hsp90 from CK2 deletion mutants
465 (YSD692, YSD675, YSD694, YSD696) and the corresponding wild type (YSD673), strains
466 were grown to mid-log phase at 30˚C in 200 ml volumes in YPD at 30˚C. Whole cell proteins
467 were extracted as described below and the C-terminally TAP-tagged chaperone was pulled
468 down using IgG agarose beads from lysate containing 20 mg of protein (see below). The
469 protein was eluted in 100 µl 1x sample buffer and heated to 95˚C for 10 minutes prior to
470 loading 30 µl onto a 10% Tris-glycine SDS-PAGE gel for separation. Coomassie-stained gels
471 were imaged and the bands corresponding to Hsp90 were cut out and processed by in-gel
472 digestion[49]. Hsp90's phosphorylation sites were identified using Glu-C and trypsin digestion
473 and liquid chromatography-mass spectrometry on a QExactive plus mass spectrometer
474 (Thermo Fisher).

475 **Structural modelling.** A model of the full-length *C. albicans* Hsp90 monomer was generated
476 based on the *S. cerevisiae* Hsp90-Sba1 crystal structure[28] (PDB #2cg9) using the Phyre[2]
477 engine[50]. The model was aligned to the *S. cerevisiae* sequence and visualized using the
478 PyMOL Molecular Graphics System[51].

479 **Ancestral character state reconstruction.** Sequences of 240 fungal taxa were obtained from
480 the Ensembl Genomes database for fungi and aligned with the murine homolog Hsp90ab1
481 (Table S4) in AliView version 1.26[52] using the integrated default alignment program
482 MUSCLE[53]. A Neighbor Joining tree was built in MEGA version 10.1.8[54] and loaded into
483 Mesquite version 3.61[55] for ancestral character state reconstruction using the parsimony
484 criterion.

485 **Western blotting and co-immunoprecipitations.**

486 To determine Hsp90 stability in the wild-type, *MAL2-HSP90* control and hsp90 mutant
487 strains, stationary phase cells grown in YPM were inoculated into YPD or YPM at an OD_{600}
488 of 0.2 and incubated until they reached a log-phase OD_{600} between 1.3 to 1.9 (approximately
489 4.5 hours). 50 ml of cell culture were pelleted, snap frozen in liquid nitrogen, and stored
490 overnight at -20˚C. Pellets were thawed on ice, washed twice with 1x PBS and resuspended in
491 250 µl lysis buffer (50 mM HEPES pH 7.5, 150 mM NaCl, 5 mM EDTA, 1% Triton X100, 1
492 cOmplete EDTA-free protease inhibitor tablet, 1 mM PMSF). Cells were transferred to
493 Precellys 2 ml Tough Micro-organism Lysing Kit tubes (VK05) and lysed using a Precellys
494 Evolution tissue homogenizer. Samples were processed in 3 cycles, each consisting of bead
495 beating at 6,000 rpm for 1 minute, pause for 30 seconds, bead beating at 6,000 rpm for 1
496 minute. Tubes were rested on ice for at least 1 minute between each cycle. Lysates were
497 cleared twice by centrifugation at 20,000 *x*g at 4˚C for 30 minutes, and 5 minutes.
498 Supernatants were transferred to microfuge tubes and refrigerated in preparation for sample
499 preparation and gel loading. The lysates' whole cell protein concentrations were determined
500 with a Quick Start Bradford Protein Assay (Bio-Rad) and calibrated against a BSA standard
501 curve. Samples were diluted to 0.1 µg/µl protein in sample buffer (70 mM Tris-HCl pH 6.8,
502 11.1% glycerol, 1.1% SDS, 0.005% bromophenol blue, 10% 2-mercaptoethanol, all final
503 concentrations), heated at 95˚C for 10 minutes and either cooled on ice prior to loading or
504 stored at -20˚C.

505 As loading controls, 100 µl per sample were loaded onto a 10% SDS-PAGE gel and
506 separated for 20 minutes at 90 volts, followed by 100 minutes at 120 volts. To visualize
507 proteins, gels were stained with SimplyBlue SafeStain (Invitrogen) according to the
508 manufacturer's instructions and imaged by scanning.

509 For immunoblotting of *C. albicans* Hsp90, 15 µl were loaded on a 10% SDS-PAGE gel
510 and separated for 20 minutes at 90 volts, followed by 100 minutes at 120 volts. Proteins were
511 wet-transferred onto a PVDF membrane (Bio-Rad) for 135 minutes at 300 mA in a Mini-
512 PROTEAN Tetra Vertical Electrophoresis Cell filled with transfer-buffer (2 M glycine, 0.25
513 M Tris-base, 20% methanol). To block free sites, membranes were treated with PBST (1x
514 PBS, 0.1% Tween 20) with 0.1% non-fat milk overnight at 4˚C. The blots were probed for 1
515 hour at room temperature with α-CaHsp90[31] diluted 1:10,000 in PBST with 0.1% milk and
516 washed with 1x PBST prior to probing with α-rabbit antibody-HRP conjugate (BioRad
517 #1705046) for 15 minutes at room temperature. Lastly, blots were washed with 200 ml PBST

518 using the SNAP i.d. 2.0 Protein Detection System (Merck Millipore), incubated with Clarity
519 Western ECL (BioRad), and imaged on the Syngene G:Box transilluminator.

520 To purify Hsp90 for mass-spectrometric analysis and to investigate the effect of Hsp90
521 phospho-mutant alleles on co-chaperone binding, 200 ml of cells were grown as described
522 above, washed twice in 1x PBS and resuspended in 2 ml co-IP lysis buffer (50 mM Tris-HCl
523 pH 7.5, 1% Nonidet P 40 Substitute (Sigma #74385), 0.25% deoxycholate Na, 150 mM NaCl,
524 5 mM EDTA, 1 mM Na_2MoO_4•$2H_2O$, PhosSTOP tablet, cOmplete EDTA-free protease
525 inhibitor tablet, 1 mM PMSF, 1 mM Na_3VO_4, and 10 mM NaF). Cells were transferred to 15
526 ml Precellys sample tubes (VWR BERT KT03961-1-4061), mixed with 1 ml acid-washed
527 glass beads (~400 µm) and mechanically disrupted using a Precellys Tissue Homogeniser.
528 Tubes were agitated three times for one minute with one minute on ice in between. The lysate
529 was cleared by centrifugation at 20,000 *x*g twice for 5 minutes at 4°C and protein
530 concentrations determined using the Bradford assay described above. 7.5 mg of protein were
531 mixed with 100 µl of IgG or α-HA agarose, depending on the strain's genotype, in co-IP
532 washing buffer (50 mM Tris-HCl pH 7.5, 1% Nonidet P 40 substitute, 0.25% deoxycholate
533 Na, 150 mM NaCl, 5 mM EDTA, 1 mM Na_2MoO_4•$2H_2O$, 1 mM PMSF, 1 mM Na_3VO_4, and
534 10 mM NaF) and gently rotated for 2 hours at 4˚C. Following precipitation, the agarose beads
535 were washed carefully 3-5 times with 1 ml co-IP washing buffer before being mixed with 100
536 µl 1x sample buffer (6x sample buffer: 0.35 M Tris HCl, 10% (w/w) SDS, 36% glycerol, 5%
537 2-mercaptoethanol and 0.012% bromophenol blue). Prior to loading, samples were heated at
538 95˚C for 10 minutes and cooled on ice ready for loading or stored at -80˚C. Proteins were
539 separated at 120 volts on size-appropriate SDS-PAGE gels.

540 To visualize epitope-tagged co-chaperones, proteins were wet-transferred onto PVDF
541 membranes for 16 hours at 20 volts in a Mini-PROTEAN Tetra Vertical Electrophoresis Cell
542 filled with transfer-buffer (2 M glycine, 0.25 M Tris-base, 20% methanol). Membranes were
543 blocked with PBST and 5% milk for at least 1 hour at room temperature before being probed
544 with primary and secondary antibodies. To visualize TAP-tagged Sti1, membranes were
545 treated with α-TAP antibody (Open Biosystems #CAB1001). Membranes carrying HA-
546 tagged Cdc37, Aha1 or Sba1 were exposed to α-HA antibody (Invitrogen #71-5500). Both
547 primary antibodies were diluted 1:5,000 in PBST with 0.2% milk and subsequently
548 conjugated with α-rabbit antibody-HRP conjugate (BioRad Immun-Star Goat Anti-Rabbit
549 (GAR)-HRP Conjugate #1705046) diluted 1:5,000. Membranes were incubated in antibody
550 solutions for 15 minutes each and washed at least three times using 1x PBST using the SNAP

551 i.d. 2.0 Protein Detection System. Lastly, proteins were visualized with Clarity Western ECL
552 (BioRad).

553 **Temperature growth profiles.** To assess susceptibility to thermal stress, optical densities of
554 stationary phase cultures were measured at 600 nm and adjusted to 0.1 in 1x PBS and serially
555 diluted two-fold. 4 µl of cell suspension were then spotted onto solid YPD or YPM and plates
556 were incubated at the indicated temperature for 48 hours. Plates were photographed and
557 analyzed visually.

558 **Cellular morphogenesis analysis.** Stationary phase cells grown in YPM at 30˚C were diluted
559 to an optical density of 0.2 in YPD or YPM and grown for 16 hours at 30˚C while shaking at
560 200 rpm. In preparation for microscopy, cells were washed and diluted with 1x PBS to a cell
561 density appropriate for microscopy. Images were collected using the DIC settings on a Nikon
562 Eclipse E8000 microscope with a Nikon Digital Sight DS-5M camera. To calculate the
563 morphology index (MI)[56], a total of 100 cells per strain were randomly selected and their
564 width at the septal junction as well as cell length and maximum diameter measured using
565 ImageJ[57]. The MI for each cell was then presented in scatter plots.

566 **Drug susceptibility assays.** Strains were grown to stationary phase at 30˚C in YPM while
567 shaking at 200 rpm and their optical densities were measured at 600 nm and adjusted to ~10^3
568 cells/100 µl. Fluconazole was diluted in water to a starting concentration of 512 µg/ml and 20
569 µl of drug were mixed with 180 µl YPD or YPM in a 96-well flat bottom dish. The drug was
570 then diluted two-fold in YPD or YPM to cover a gradient ranging from 256 µg/ml to 4 µg/ml.
571 100 µl of cell suspension were added to each well and plates were incubated for 48 hours at
572 25˚C and optical densities recorded at 595 nm. A 5 mM radicicol stock solution (DMSO) was
573 diluted to 50 µg/ml in YPM or YPD. The drug was diluted in either media to the following
574 concentrations: 1, 2, 3, 4, 5, 7.5, 10, 15, 20, and 25 µg/ml and strains inoculated as above. To
575 account for the effects of DMSO alone, strains were also inoculated in 0.0275% DMSO.
576 Plates were incubated for 48 hours at 25˚C in the dark and optical densities recorded at 595
577 nm. Optical density values were normalized to the no treatment column and visualized using
578 Java TreeView version 1.1.6r4[58].

579 **Colony morphology screen.** Wild-type, control and mutant strains were grown overnight in
580 YPM at 30˚C while shaking at 200 rpm. Stationary cultures were then diluted to an optical
581 density of 0.02 at 600 nm and 5 µl of cell suspension spotted onto RPMI, Spider, and
582 synthetic defined media with and without Calcofluor White or Congo Red (Table S5). After

583 incubation at 30˚C for 48 hours colonies were visually scored for appearance as 'smooth',
584 'rough', 'wrinkly', or 'wrinkly with hyphal edge' and photographed.

585 **Biofilm analyses.** In preparation for biofilm analyses, *C. albicans* strains were cultured
586 overnight in YPD at 30˚C while shaking at 150 rpm. Stationary phase cells were centrifuged
587 at 4,400 rpm for 5 minutes, washed with 1x PBS and counted using a Neubauer
588 hemocytometer. To induce biofilm formation, cells were diluted to 10^6 cells/ml in RPMI
589 (Sigma-Aldrich/Merck # R7755) and incubated at 37˚C for 24 hours in flat-bottom 96-well
590 dishes for cell viability and biomass assays or on Thermanox™ coverslips for scanning
591 electron microscopy. Cell viability was assessed by metabolic reduction of resazurin sodium
592 salt (Sigma-Aldrich/Merck #R7017). For the assay, 0.1 g of resazurin was dissolved in 10 ml
593 1x PBS and filter-sterilized. Biofilm wells were washed twice with 1x PBS and filled with
594 100 µl of a 1:1000 dilution of resazurin in RPMI. Plates were incubated at 37˚C for 25
595 minutes and absorbance measured at 570 nm. Upon completion of the resazurin cell viability
596 assay, plates were left to dry overnight and biofilm biomass assessed by staining with 0.05%
597 w/v crystal violet. Upon washing and de-staining with 100% ethanol, biomass was quantified
598 by spectrophotometric measurements at 570 nm in a FluoStar Omega (BMG Labtech)
599 microtitre plate reader[59]. To visualize biofilms grown on coverslips, they were washed once
600 with 1x PBS and fixed overnight at 4˚C in 500 µl of 0.15% w/v Alcian Blue dissolved in 2%
601 para-formaldehyde, 2% glutaraldehyde, and 0.15 M sodium cacodylate. Samples were imaged
602 as described previously[60].

603 **Virulence assays.** To assess if Hsp90 phosphorylation affects virulence, we infected
604 caterpillars of the Tobacco Hornworm *Manduca sexta*[38], a novel invertebrate model of fungal
605 disease. In preparation for virulence assays, *C. albicans* strains were grown overnight in YPD
606 at 30˚C and stationary phase cultures were washed twice with 1x PBS. Cell density was
607 adjusted to 10^8 cells/ml for each strain and groups of ten caterpillars were injected with 100 µl
608 cell suspension per animal or 1x PBS in their left rear proleg. Caterpillars were maintained at
609 37˚C and scored for survival after 16 hours.

610 **Statistical analyses.** All analyses were carried out in R Version 3.6.0 and plotted using
611 ggplot2. To assess the effect of the Hsp90 mutant alleles on cellular morphology, the MIs for
612 samples grown in YPD and YPM were compared with each other using the Mann-Whitney U
613 test. Statistical differences between biofilm cell viability and biomass production were
614 assessed using a linear model of strain versus optical density comparing the mutant strains to

615 the maltose control. Statistical significance of caterpillar survival was assessed using Fisher's
616 exact test.
617

Acknowledgments

We would like to thank Prof Alistair J. P. Brown for comments on the manuscript, Ewan Basterfield and Chris Apark for technical support with the *Manduca* caterpillars, and Profs Julia R. Köhler, Jürgen Wendland, and Malcolm Whiteway for their generous plasmid gifts. This work was funded by MRC grant MR/L018349/1 to SD. JLC was supported by the MRC GW4 'Biomed' Doctoral Training Program.

Author contributions

LA, JLC and SD conceived and designed this study. LA constructed strains, prepared samples for mass spectrometry, conducted Hsp90 stability assays and assessed co-chaperone associations. JLC conducted Hsp90 stability and drug susceptibility assays. UO performed the structural modelling analysis. RW performed Hsp90 phylogenetic analyses and ancestral character state reconstruction. CEW performed *in vivo* assays. HOB analyzed growth, morphology, and biofilm data. CS assisted with mass spectrometric analyses. MB & GR performed and analyzed biofilm formation. SD drafted and edited the manuscript.

Competing interest declaration

The authors declare no competing interests.

Additional information

Supplementary information is available for this paper.

Correspondence and requests for materials should be addressed to SD.

Code availability: All custom code is available from:
https://github.com/hobrien/DiezmannLab/blob/master/T25_analysis.Rmd

Corresponding author: Stephanie Diezmann s.diezmann@bristol.ac.uk

644 **Figures**

Alaalm et al. **Figure 1**

a

T25 S530

Candida albicans	ISQLMSLIIN**T**VYSNKEIFLR ... ITKD-FELEE**S**DEEKAAREKE
Saccharomyces cerevisiae	ITQLMSLIIN**T**VYSNKEIFLR ... ITKD-FELEE**T**DEEKAEREKE
Drosophila melanogaster	IAQLMSLIIN**T**FYSNKEIFLR ... VTKEGLELPE**D**ESEKKKREED
Caenorhabditis elegans	IAQLMSLIIN**T**FYSNKEIFLR ... VTKEGLELPE**T**EEEKKKFEED
Homo sapiens	IAQLMSLIIN**T**FYSNKEIFLR ... VTKEGLELPE**D**EEEKKKQEEK
Arabidopsis thaliana	INQLMSLIIN**T**FYSNKEIFLR ... ATKEGLKLEE**T**DDEKKKKEEL

high similarity (≥90%) low similarity (≥50%) no similarity

b

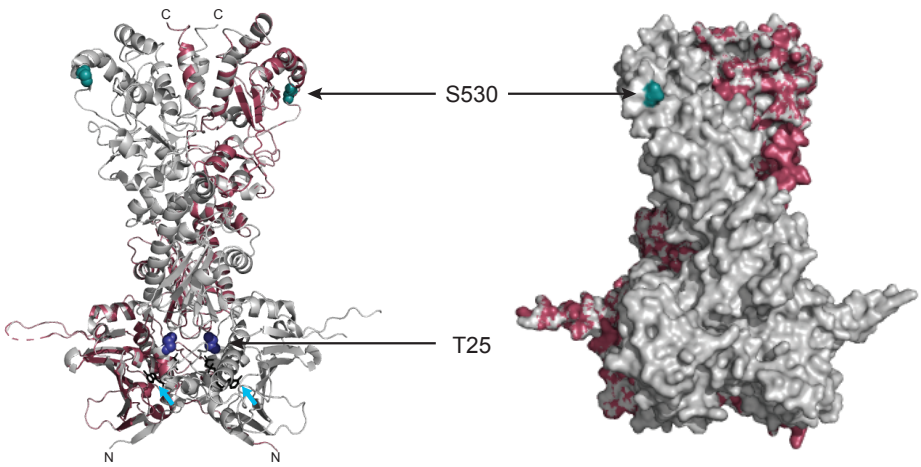

c

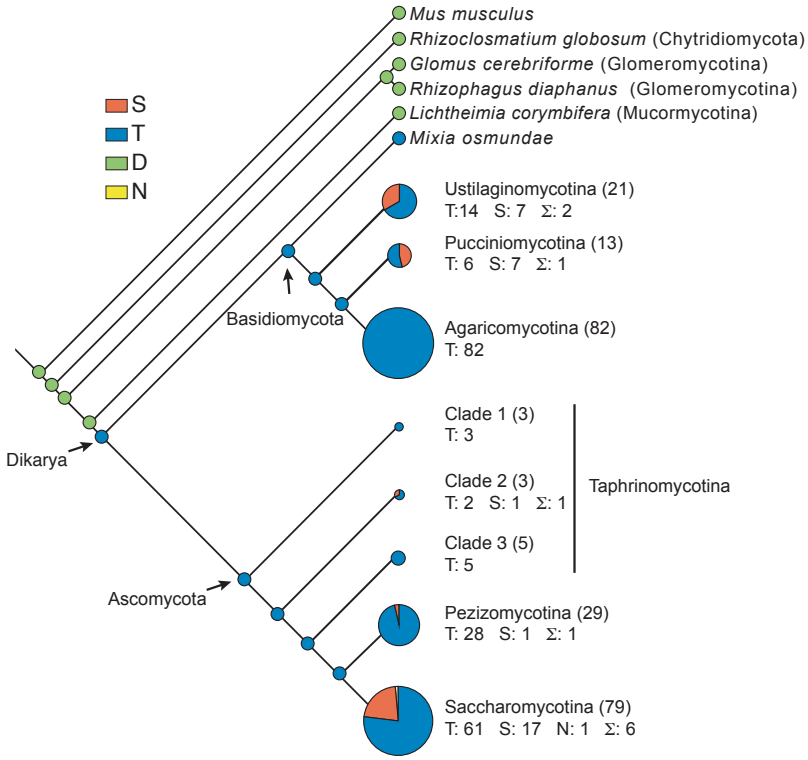

645

646 **Figure 1: Structural modeling and ancestral character state reconstruction of CK2**
647 **phosphorylation sites in Hsp90.** a) Alignment of eukaryotic Hsp90 protein sequences,
648 comparing two fungal sequences to three animal and one plant protein. T25 resides in a
649 highly conserved (red) region of the N-terminal domain of Hsp90. S530 is located in a
650 divergent (blue) region of the Hsp90 middle domain. b) *C. albicans* Hsp90 (purple) modeled
651 on the full-length crystal structure of *S. cerevisiae* Hsp90 (grey). T25 (blue) and S530 (teal)
652 are visualized on the homology model (left) and the surface model (right). Azure arrows point
653 to bound ATP in the homology model. c) Ancestral character state reconstruction of
654 $Hsp90^{S530}$ in 240 fungal taxa reveals at least eleven independent transitions from threonine
655 (blue) to serine (red) within the Dikarya. Basal fungi share the ancestral aspartic acid residue
656 (green) with the animal root (*Mus musculus*) of the tree. Within the Ascomycota and the
657 Basidiomycota, subphyla have been collapsed and the circle size indicates the number of taxa
658 within each clade. The number of taxa per subphylum is given in brackets, and the number of
659 taxa with either threonine or serine or asparagine (yellow) are indicated with T, S, or N. The
660 number of independent transitions within each subphylum is indicated by Σ. For character
661 state reconstruction within ascomycetous and basidiomycetous subphyla see Fig. S1.
662

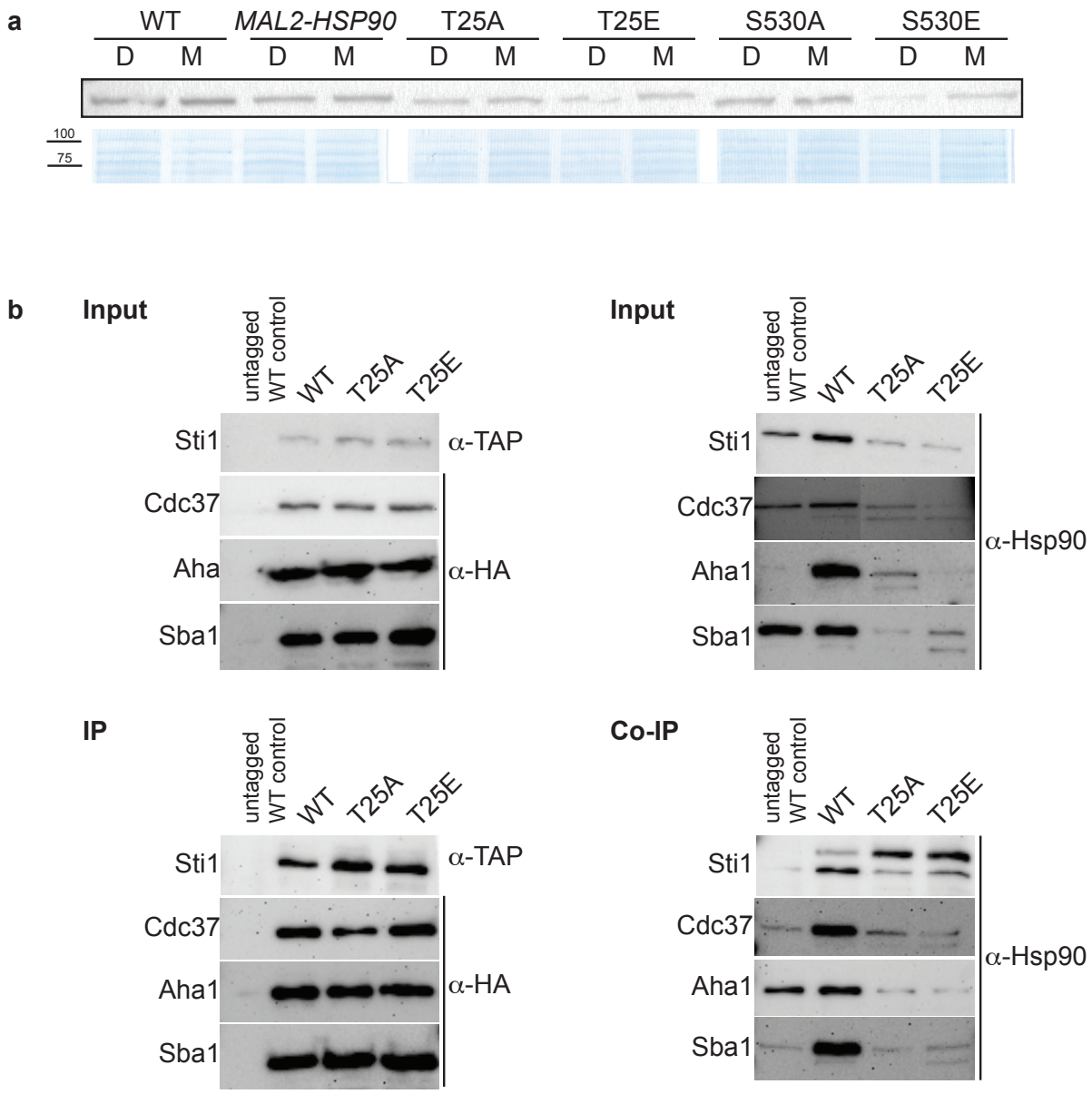

Figure 2: The *C. albicans* Hsp90 co-chaperone machinery is regulated by phosphorylation. a) One of two Western blots probed for presence of Hsp90 in *C. albicans* wild-type (WT), promoter control (*MAL2-HSP90*) and T25 and S530 mutant strains (top). Strains were grown in media containing either maltose (M) or dextrose (D) to regulate expression of mutant *HSP90* via the maltose-inducible promoter. A Coomassie-stained SDS gel validates equal loading of protein samples (bottom). b) TAP-tagged Sti1 and HA-tagged co-chaperones Cdc37, Aha1, and Sba1 were co-immunoprecipitated with Hsp90 in the wild type (WT) and the T25 mutants. The input was first probed for presence of co-chaperones and Hsp90 prior to immuno-precipitation with IgG or α-HA agarose targeting the co-chaperones.

673 Levels of co-chaperones were then assessed in the immuno-precipitate (IP) using α-TAP and
674 α-HA antibodies. To screen for co-immunoprecipitated Hsp90 (Co-IP), the membrane was
675 probed with an Hsp90-specific antibody.
676

Figure 3

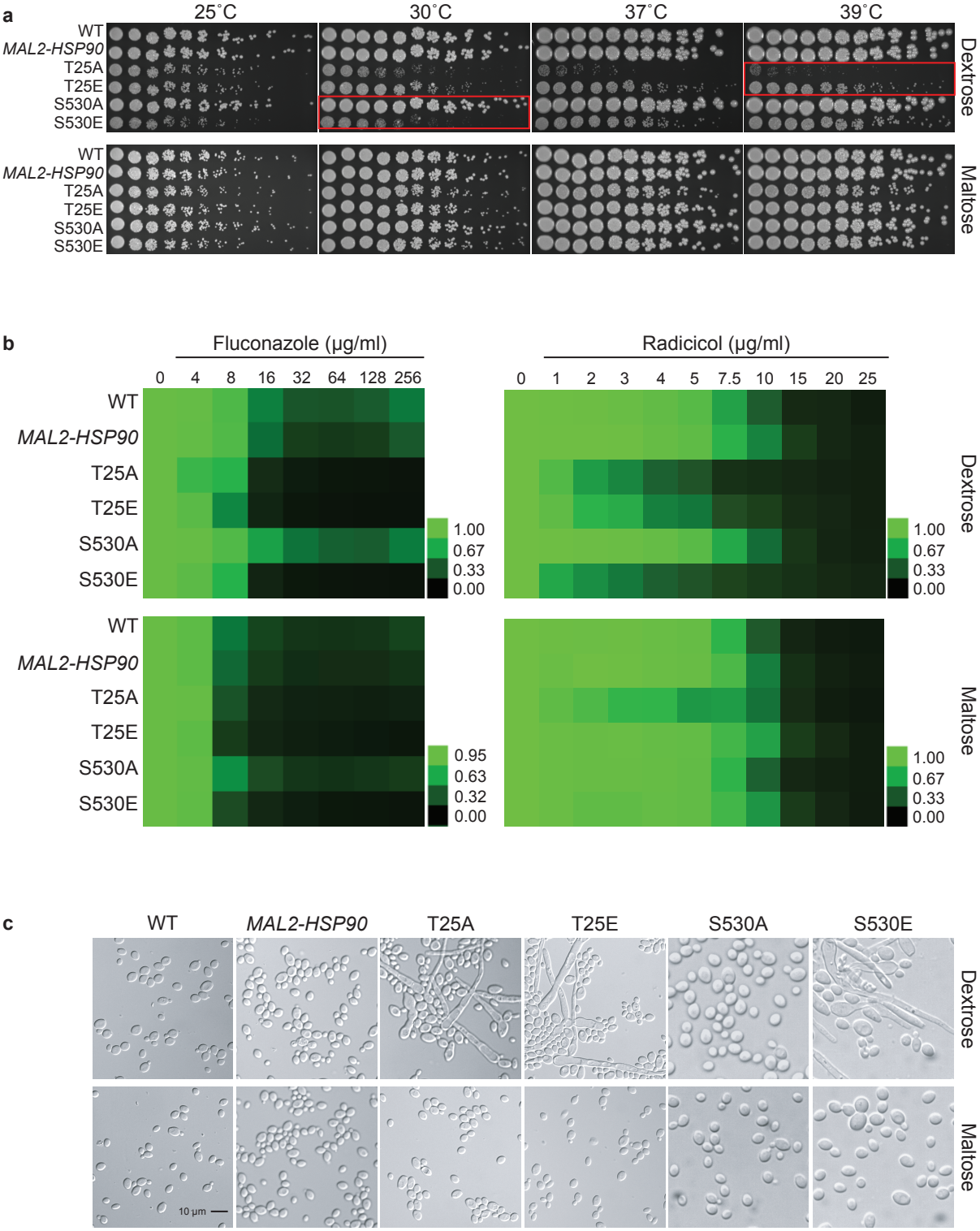

677

678 **Figure 3: Expression of key virulence traits is contingent on Hsp90's phosphorylation**
679 **status.** a) Two-fold serial dilutions of the *HSP90* wild-type, the *MAL2-HSP90* promoter
680 control strain, and *hsp90* phospho-mutants were spotted onto solid media containing either
681 dextrose or maltose and incubated at the indicated temperatures for 48 hours. Red boxes

682 highlighting severe phenotypes. b) Wild-type and mutant cells were exposed to increasing
683 doses of the commonly employed antifungal drug fluconazole and the Hsp90 inhibitor
684 radicicol in media containing either dextrose (top) or maltose (bottom). Following incubation
685 at 25˚C, cell growth was assessed, normalized to the media only control and expressed as heat
686 map where green indicates full growth and black represents no growth. c) DIC microscopic
687 images of representative cells from each strain confirming morphogenetic changes of cells
688 grown in dextrose (top) but not maltose (bottom). Shown are one of two biological replicates.
689

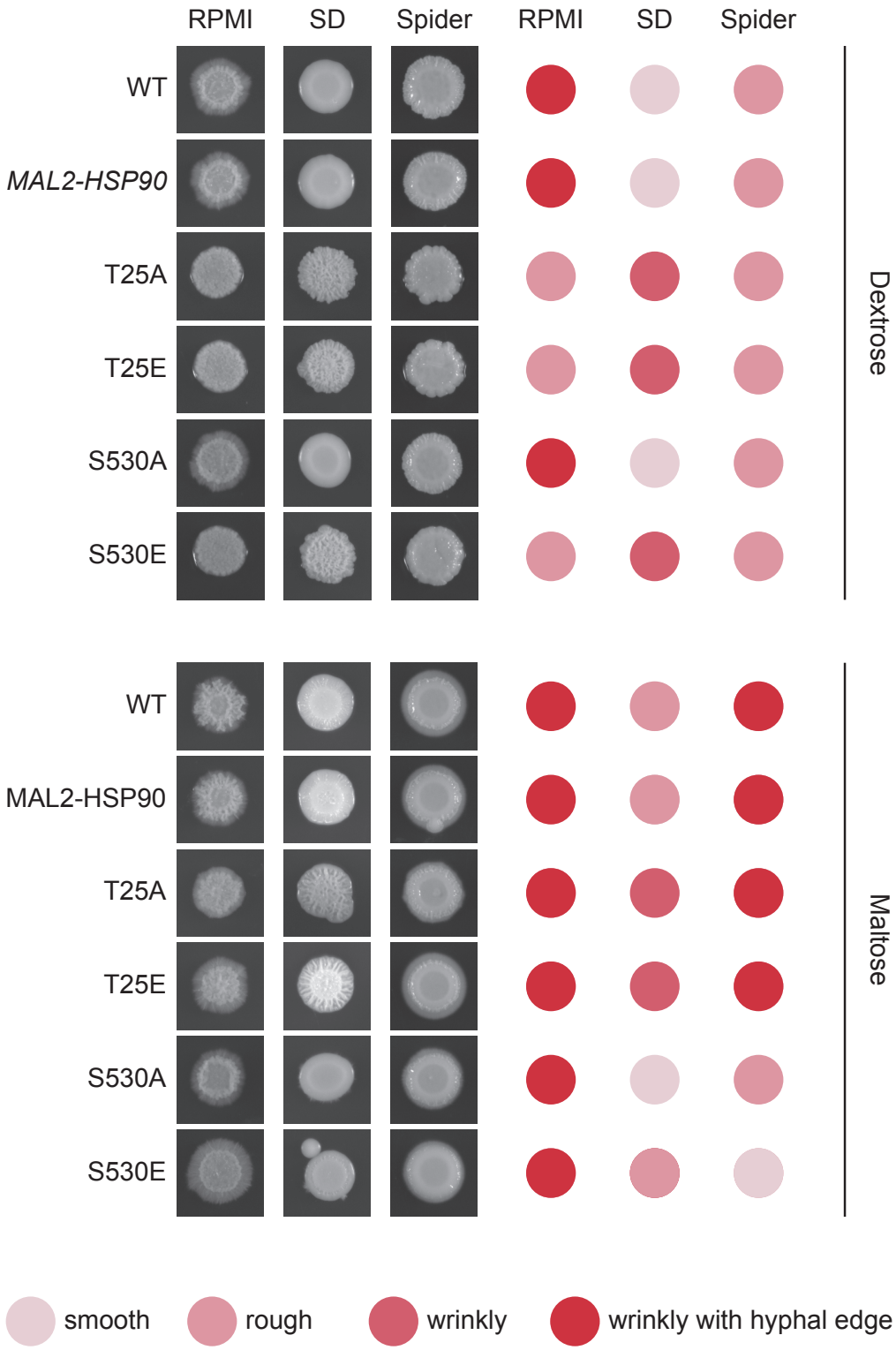

690

691 **Figure 4: Aberrant colony morphology in response to changes in Hsp90 phosphorylation**
692 **patterns.** Images of colonies spotted onto RPMI, Spider or synthetic defined (SD) media
693 containing either dextrose (top) or maltose (bottom). Colonies were scored for their

694 appearance. The darker red the dot, the more extreme the colony phenotype. Shown is one of
695 two replicates.
696

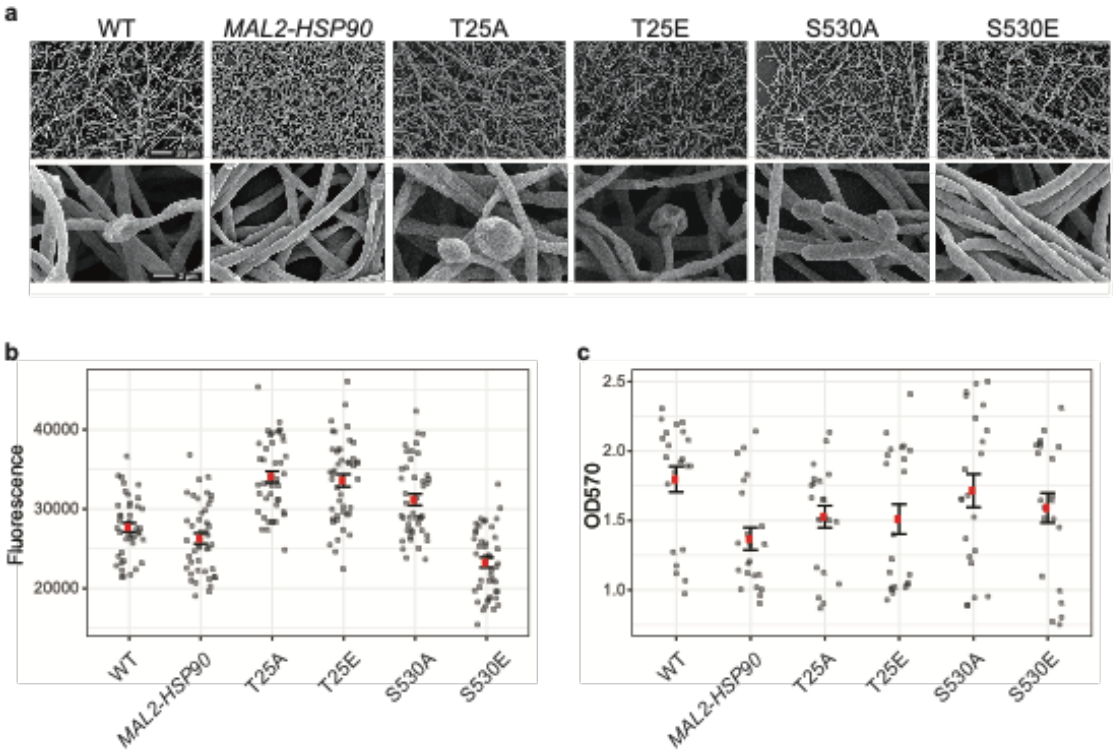

Figure 5: Biofilm architecture remains unaffected by Hsp90 phosphorylation. a) Scanning electron microscopy images of mature biofilms at 800x (top) and 8,000x (bottom) magnification reveal biofilm architecture between the wild type, the control and the phospho-mutants to be indistinguishable upon visual inspection. b) Biofilm cell viability, measured as fluorescence for 44 replicates per strain, is significantly reduced in strain S530E. c) Metabolic biomass measurements for 22 replicates per strain as absorption at OD_{570} were comparable to the promoter control.

706 **Table 1: Patterns of Hsp90 phosphorylation (P) detected in the wild type (WT) and the**
707 **CK2 mutants.**

	C. albicans genotypes				
Hsp90 site	WT	*cka1*Δ/Δ	*cka2*Δ/Δ	*ckb1*Δ/Δ	*ckb2*Δ/Δ
S279	-	P	-	-	-
S294	P	P	P	P	P
S530	P	P	-	P	-

708